

## Headline Articles

---

### Reaction Mechanism of the Pyrolysis of Polycarbosilane and Polycarbosilazane as Ceramic Precursors

Masaki Narisawa,\* Manabu Shimoda, Kiyohito Okamura, Masaki Sugimoto,<sup>†</sup> and Tadao Seguchi<sup>†</sup>

Department of Metallurgy and Materials Science, College of Engineering, University of Osaka Prefecture, Sakai, Osaka 593

<sup>†</sup>Takasaki Radiation Chemistry Research Establishment, Japan Atomic Energy Research Institute, Takasaki, Gunma 370-12

(Received November 14, 1994)

The pyrolytic processes of polycarbosilane (PCS) to silicon carbide and of polycarbosilazane (PCSZ) to silicon carbonitride were studied by gas analysis, electron spin resonance (ESR), and X-ray diffraction. On the progress of conversion from organic polymers to ceramics above 800 K, decomposition gases like CH<sub>4</sub> and H<sub>2</sub> evolved, and free radicals as the intermediate active species in the chemical reactions were detected during the pyrolysis. The gas yield and the radical concentration profile against pyrolysis temperature indicated that there were several steps in the pyrolysis of PCS and PCSZ. At the last step in the pyrolysis of PCS, the microcrystals of  $\beta$ -SiC began to precipitate, while the microcrystals of  $\beta$ -SiC and Si<sub>3</sub>N<sub>4</sub> precipitated in the pyrolysis of PCSZ.

Polymer fibers have been used as the precursor for ceramic fibers. At present, silicon carbide fiber is synthesized from polycarbosilane (PCS), and several types of silicon carbonitride fibers are also synthesized from polycarbosilazane (PCSZ) or PCS fiber.<sup>1,2)</sup> In these methods, the precursor fibers are converted into those ceramic fibers by the pyrolysis at high temperatures. The reaction mechanism in the pyrolysis, however, has not been clear, though it should be important to control the conversion process and improve the properties of the resultant ceramics.

The silicon carbide fiber prepared from PCS has been known to have desirable properties for reinforcement of the ceramics matrix composites designed for high temperature use.<sup>3,4)</sup> Since the properties of this fiber depends on the pyrolysis process of PCS fiber, its pyrolytic reaction has been investigated with various techniques, such as nuclear magnetic resonance (NMR), infrared spectroscopy (IR), electron spectroscopy for chemical analysis (ESCA), and others.<sup>5,6)</sup> The conversion process of PCSZ into inorganic ceramics is also important and has been well studied in recent years.<sup>7–9)</sup>

The article describes the chemical reactions during the pyrolysis of PCS and PCSZ together with the

changes in microstructure of pyrolyzed products on the basis of analysis of evolution gas and free radicals formed.<sup>10–12)</sup> Since these polymers were not cured before pyrolysis, their chemical reaction in the pyrolysis was found to be a little different from that of the cured polymers. The gas components, yields, and the radical concentration were analyzed at various heat treatment temperatures, and the ceramics obtained were analyzed by X-ray diffraction to evaluate their crystal structure.

#### Experimental

**Materials.** PCS, supplied from Shin-Etsu Chemical Co., Ltd., was  $2.0 \times 10^3$  dalton in molecular weight and about 508 K of melting temperature. Its chemical composition was Si:C:H:O=1:1.93:4.71:0.01. PCSZ, supplied from Chisso Chemical Co., Ltd., was  $1.0 \times 10^3$  dalton in molecular weight and 373 K of melting temperature. Its chemical composition was Si:C:N:H=1:1.04:1:3.51 in spite of a small amount of oxygen retained. These PCS and PCSZ were used in grain form in the following experiments.

**Gas Analysis.** Each polymer of about 0.5 g was put in a sample tube, and the tube was heated up to a constant temperature after evacuation. The heating rate was 10 K min<sup>-1</sup>, and the tube was held for 30 min at the first heat treatment temperature of 500 K. The gases accumu-

lated in the tube were analyzed using a gas chromatograph (Hitachi Gas Chromatograph 163) at room temperature. After this gas analysis, the same sample tube was evacuated and heated again at a temperature 100 K higher than the first heat treatment. The heating rate was  $20 \text{ K min}^{-1}$  up to the first heat treatment temperature and was slowed down to  $10 \text{ K min}^{-1}$  for reaching the higher temperature. The accumulated gases were then analyzed by the same method. These procedures were repeated up to 2000 K. The details of the gas chromatography were reported in our previous papers.<sup>10,11)</sup>

**Free Radical Detection by ESR.** A polymer sample of about 1 g was heated up to 400–2000 K in an argon gas flow with a heating rate of  $5 \text{ K min}^{-1}$ . After keeping it for 30 min at a fixed temperature, the sample was rapidly cooled down to room temperature. For ESR measurement, the heat treated sample of about 3 mg was put in a quartz tube of 3 mm in diameter. ESR spectrum was observed at room temperature in air using an X-band spectrometer (JEOL-FE3X). The spectrum was recorded as differential curve with applying a 100 kHz field modulation. The free radical yield was measured from ESR signal intensity by comparing with the ESR spectrum of a standard sample (TEMPO: 2,2,6,6-tetramethyl-1-piperidinyloxy).

**X-Ray Diffraction (XRD).** The X-ray diffraction (XRD) was measured for the same sample used for the ESR measurement on an X-ray spectrometer (Rigaku RINT-5000). The X-ray was generated at 40 kV and 20 mA, and the  $\text{Cu K}\alpha_1$  radiation was used.

## Results and Discussion

**Pyrolysis of PCS.** Figure 1 shows the amounts of evolution gases of hydrogen ( $\text{H}_2$ ), methane ( $\text{CH}_4$ ), and carbon monoxide ( $\text{CO}$ ) during the pyrolysis of the uncured PCS between 400–2000 K. The major gases are  $\text{H}_2$  and  $\text{CH}_4$  as observed in the pyrolysis of the cured PCS fibers.<sup>10,11,13)</sup> The  $\text{H}_2$  evolution is seen in a broad temperature range, with a peak at 900 K, a shoulder at 1200 K, and a broad tail until 2000 K.

There should be several steps in the decomposition

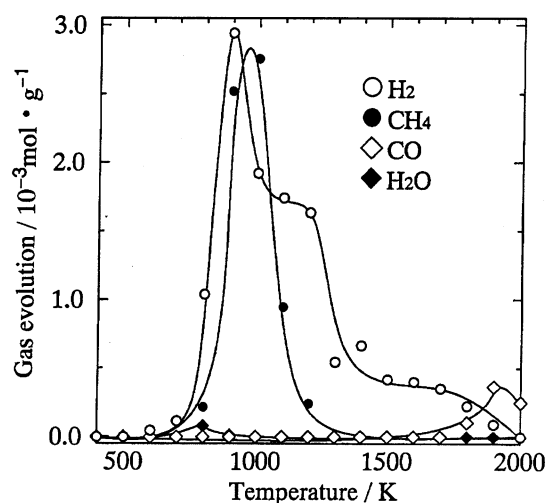


Fig. 1. Gas evolution during pyrolysis of the uncured PCS.

reaction of PCS judging from the  $\text{H}_2$  evolution. The peak of  $\text{H}_2$  evolution at 900 K accompanied by the peak of  $\text{CH}_4$  evolution at 1000 K may correspond to the bond cleavage at the Si atoms in PCS, that is, Si–H and Si– $\text{CH}_3$  ruptures. The shoulder of  $\text{H}_2$  evolution at 1200 K corresponds to the bond cleavage at meth-

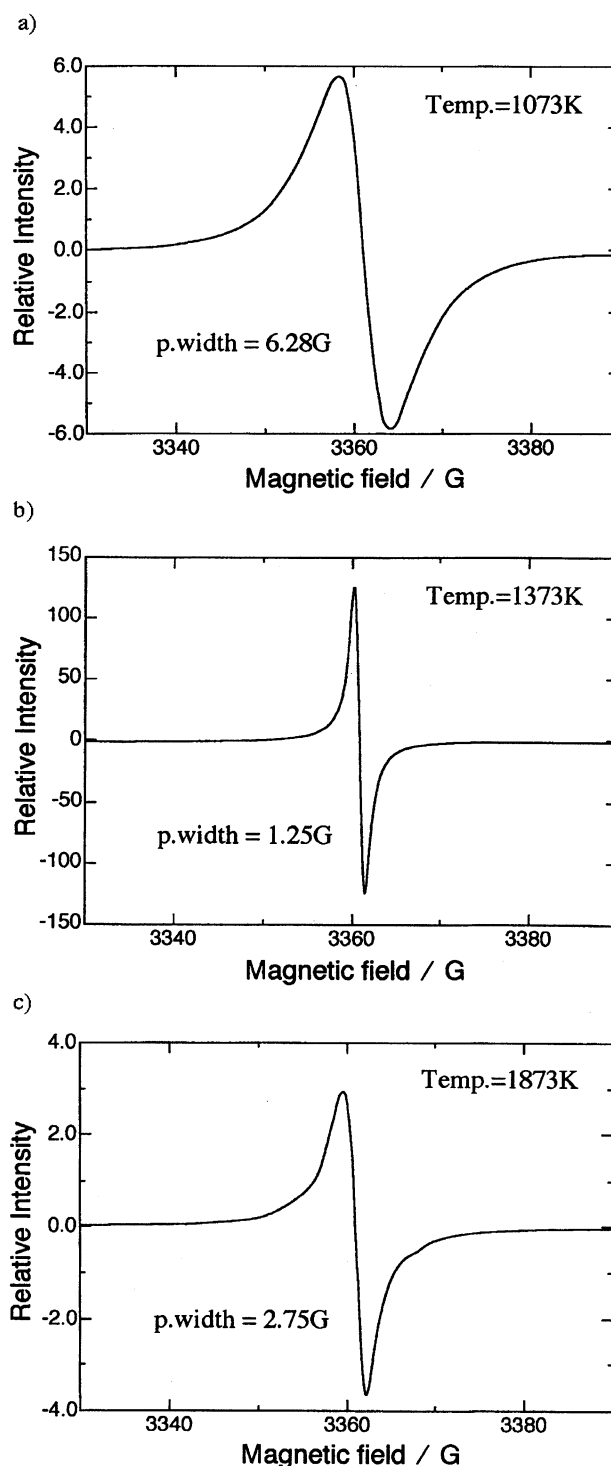


Fig. 2. ESR spectra observed at room temperature for PCS pyrolyzed at various temperatures. a) at 1073 K, b) at 1373 K, c) at 1873 K.

ylene ( $-\text{CH}_2-$ ) groups in PCS chains. Since the bond energy of C-H is larger than that of Si-H.<sup>14)</sup> Their decomposition temperature is thought to be higher in the order of bond energy. These behaviors are very similar to those in the pyrolysis of the radiation-cured PCS fibers.<sup>10,11)</sup> The characteristic broad tail of the  $\text{H}_2$  evolution around 1600–2000 K was not observed in the pyrolysis of the cured fibers and is specific to the uncured PCS. It should be attributed to the rupture of C-H bond remaining in the pyrolyzed products. The cured PCS maintains its shape and specific surface area does not change remarkably during the pyrolysis, while that of the uncured PCS changes with the temperature. This should be one of the reason why the amount of the gas evolution from PCS is influenced by the curing.

Above 1800 K, a small amount of CO gas evolved, which should be due to the decomposition of Si-O-Si or Si-O-C structure remaining in the pyrolyzed product.<sup>15)</sup> These contaminant oxygen atoms had been introduced into PCS by capping reaction of the groups during the polymerization of dichlorodimethylsilane.

Traces of ethane and ethylene gases ( $10^{-5}$ – $10^{-6}$  mol  $\text{g}^{-1}$ ) were also detected by the gas analysis. They evolved at almost the same temperature occurring the evolution of methane gas.

By the above bond cleavages in the pyrolysis, free radicals should be formed as an intermediate active species. A part of the radicals can be trapped in the matrix cooled down to room temperature.<sup>10,11,16)</sup> Figure 2 shows the electron spin resonance (ESR) spectra observed at room temperature for the products pyrolyzed at 1073, 1373, 1873 K. Each signal is a singlet line. The  $g$ -factor is 2.0028–2.0030 which is almost the same as that of the free radical formed in an organic PCS by  $\gamma$ -ray irradiation at 77 K or room temperature.

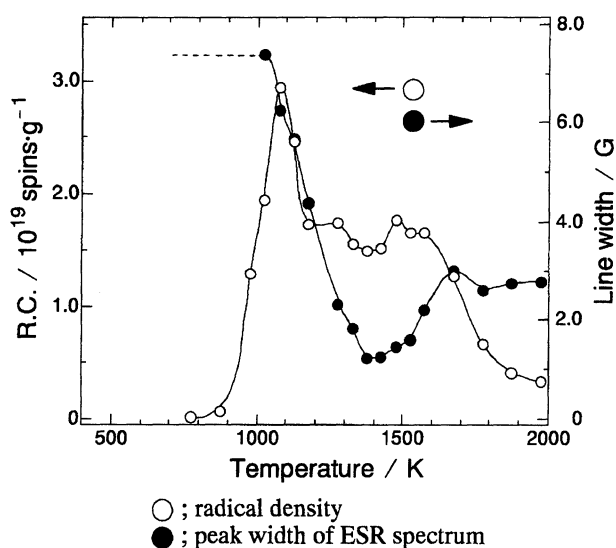


Fig. 3. Radical concentration and ESR signal line width (Peak-Peak) vs. pyrolysis temperature for PCS.

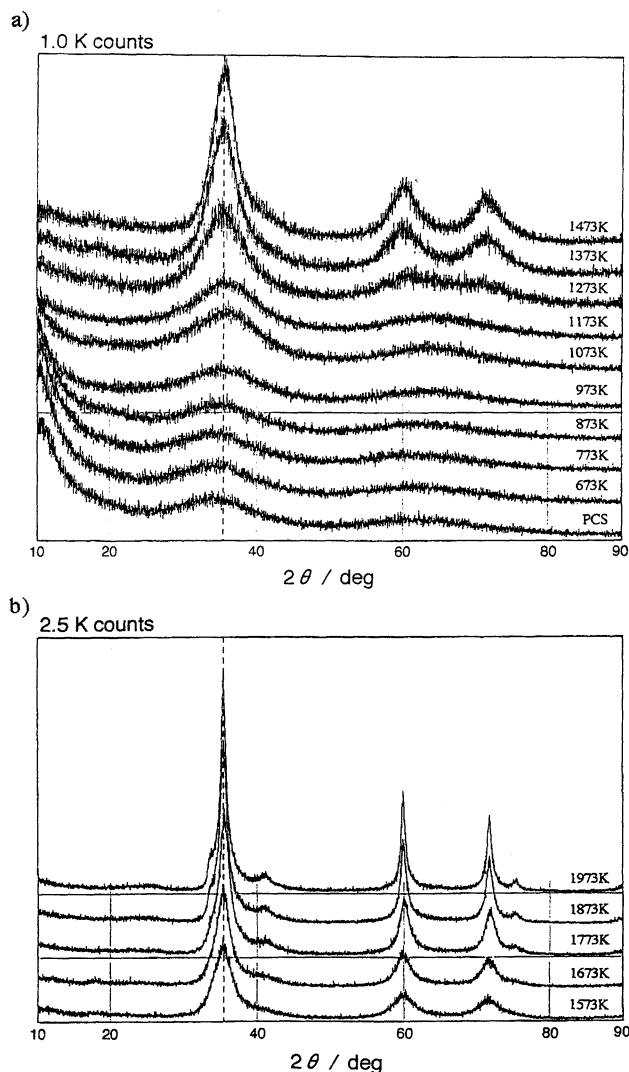


Fig. 4. X-Ray diffraction patterns of the pyrolyzed PCS at various temperatures. a) from 673 to 1473 K, b) from 1473 to 1973 K.

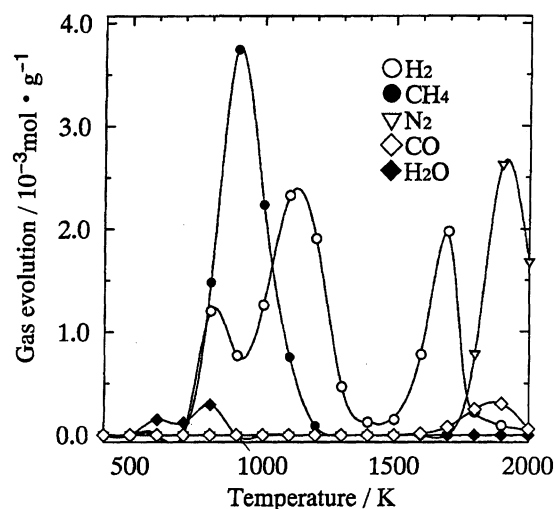


Fig. 5. Gas evolution during pyrolysis of PCSL.

The radical species formed around 1000 K and above 1200 K are assigned to Si- and C-sited free radicals, respectively. The changes in ESR spectrum with heat treatment temperature were monitored by the line width, i.e., the peak to peak separation of the ESR signals in Fig. 2. The radical concentration was also calculated from the ESR signal intensity by comparing with that of TEMPO.

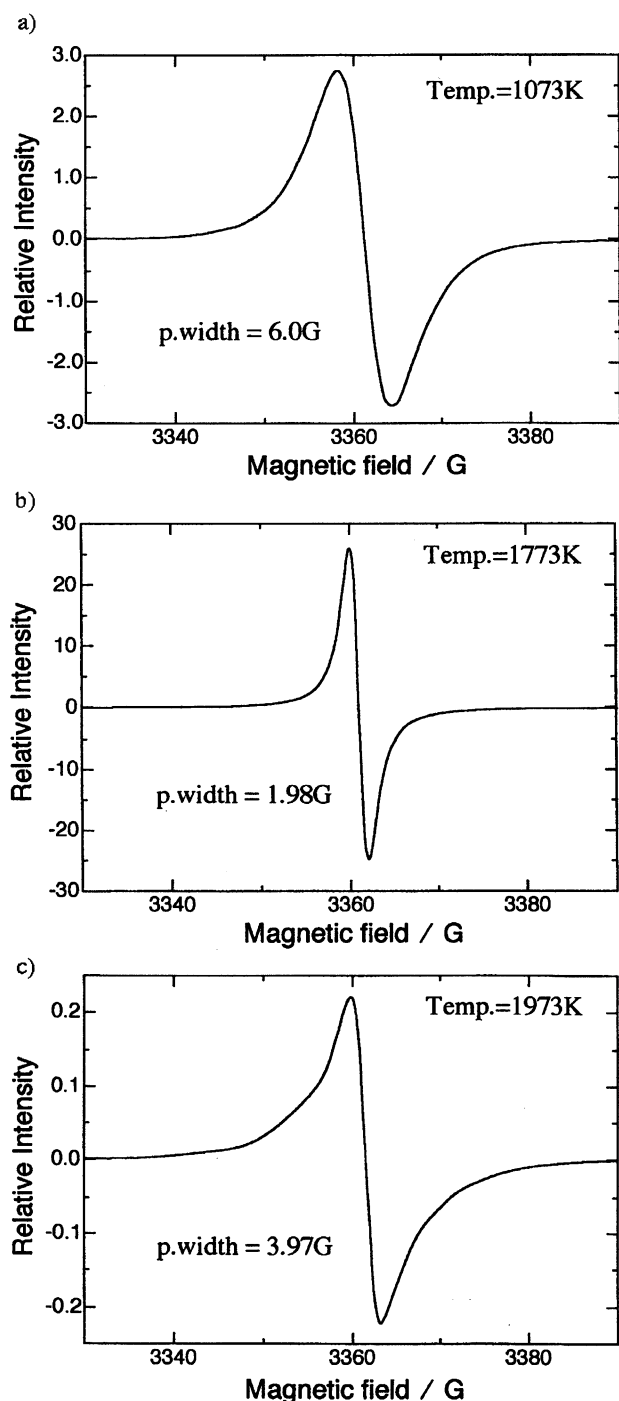


Fig. 6. ESR spectra observed at room temperature for PCSL pyrolyzed at various temperatures. a) at 1073 K, b) at 1773 K, c) at 1973 K.

Figure 3 shows the change of line width and radical concentration as a function of the heat treatment temperature for PCS. The line width decreases sharply in the temperature range of 1000–1300 K, then slightly increases at the higher temperature. It means that the radical species would change with the progress of pyrolysis. The Si-sited radicals with H atoms neighboring C atoms are formed at the lower temperature and lose the neighboring H atoms with a rise of temperature to be replaced by C-sited radicals at the higher temperature. The radical concentration increases greatly above 900 K, and reached the maximum at 1000 K, and then decreased with a rise of temperature to 1100 K. It was kept constant and turned to decrease above 1500 K. The Si-sited radicals may be formed around 1000 K and trapped in the solid matrix, while the C-sited radicals may be formed and trapped above 1200 K.

The profile of the radical concentration is quite similar to that of  $H_2$  evolution (Fig. 1). Therefore the observed radicals, which are trapped stably in the matrix, would be closely related to the rupture of Si–H and C–H bonds. Most of the radicals should react with each other at the pyrolysis temperature, but some could survive and remain in the cooled matrix. Of course, the radicals would be produced by the ruptures of Si–CH<sub>3</sub>, Si–O, and C–O with the gas evolution of CH<sub>4</sub> and CO. The effect of ruptures of these chemical groups on the profile of the trapped radical concentration is, however, small as compared with the rupture of Si–H and C–H.

Figure 4 shows the changes in the XRD pattern of the pyrolyzed product with heat treatment temperature.<sup>5,6)</sup> A dotted line in Fig. 4 (35.6°) indicated the (111) diffraction of  $\beta$ -SiC single crystal reported in literature. Original PCS showed broad diffraction peaks around  $2\theta = 35^\circ$  and  $65^\circ$ . The peak around  $2\theta = 35^\circ$  shifted

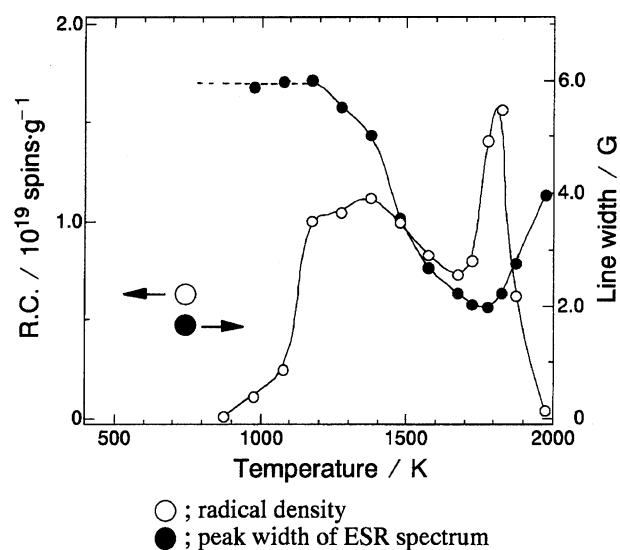


Fig. 7. Radical concentration and ESR signal line width (Peak–Peak) vs. pyrolysis temperature for PCSL.

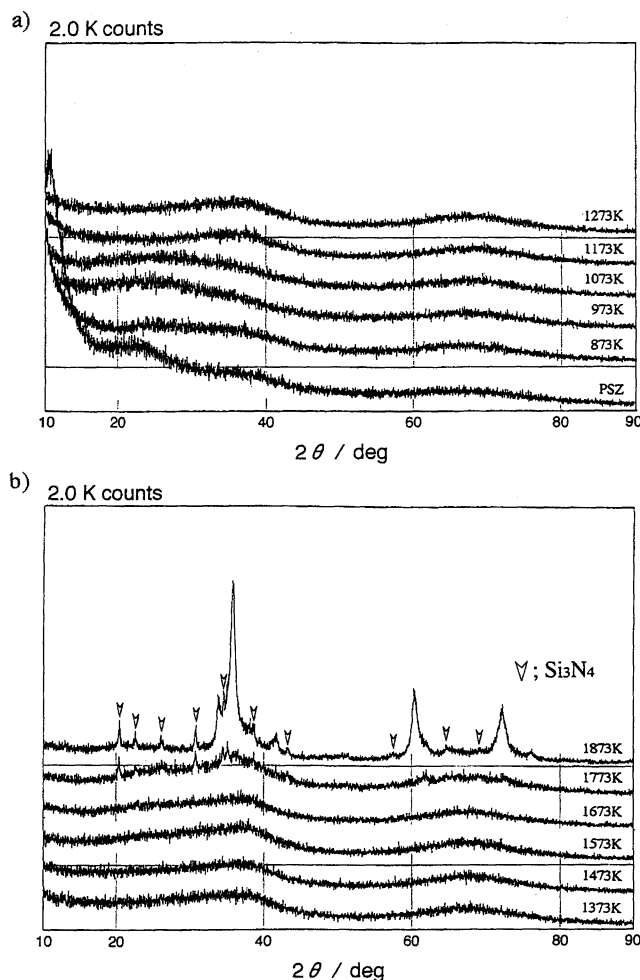


Fig. 8. X-Ray diffraction patterns of the pyrolyzed PCSL at various temperatures. a) from 873 to 1273 K, b) from 1373 to 1873 K.

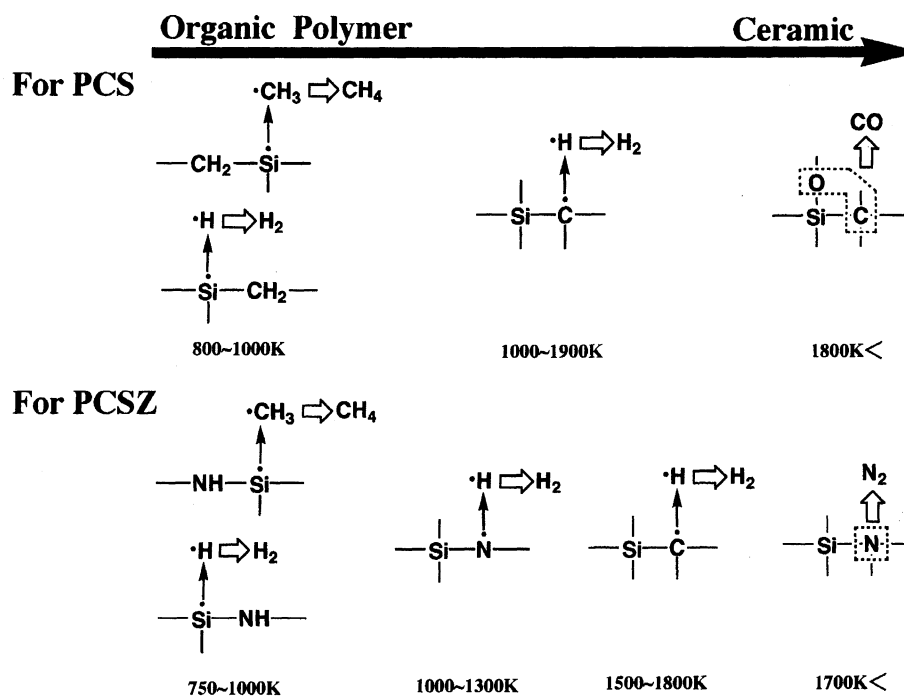


Fig. 9. Reaction mechanisms of PCS and PCSZ during pyrolysis.

to a higher angle as the heat treatment temperature increased, exceeding  $35.6^\circ$  at 1073 and 1173 K. The peak angle, however, turned back again to  $35.6^\circ$  at 1273 K. Above 1373 K, the broad peak around  $65^\circ$  began to split. These results in the XRD measurement indicate that  $\beta$ -SiC microcrystals begin to precipitate from amorphous matrix consisting of Si, C, O, and H in the range of 1273–1373 K. In this temperature range, the  $H_2$  evolution from PCS decreases suddenly as shown in Fig. 1. Therefore, the precipitation of  $\beta$ -SiC crystals is considered to occur just after the decomposition of C–H bond of methylene groups.

**Pyrolysis of PCSZ.** Figure 5 shows the profiles of the gas evolution from PCSZ when pyrolyzed at 400–2000 K. The  $CH_4$  evolution has one peak at 900 K. The  $H_2$  evolution has three peaks at 800, 1100, and 1700 K. The  $N_2$  evolves at high temperature above 1700 K. A small amount of CO also evolves above 1700 K.

The  $CH_4$  evolution is assigned to the decomposition of Si– $CH_3$  bond, and the  $H_2$  evolution at 800–900 K is assigned to the decomposition of Si–H bond as observed for PCS. The  $H_2$  evolution around 1100 K would correspond to the decomposition of N–H and C–H bonds, and the  $H_2$  evolution around 1700 K is also thought to be due to the decomposition of C–H bonds. The amount of  $H_2$  produced from PCSZ at high temperatures is larger than that from PCS. The inorganic network formed with the PCSZ pyrolysis should have different composition and properties from that formed with the PCS pyrolysis. The  $N_2$  and CO evolutions, having a peak at 1900 K, would correspond to the decomposition of the amorphous phase consisting of Si, C, N, O, and H, and the precipitation of microcrystals.

Figure 6 shows the ESR spectra of PCSZ after the pyrolysis at 1073, 1773, and 1973 K. Each signal is single line, and its  $g$ -factor is about 2.003. The line width (peak–peak distance) and the intensity of the signals depend on the pyrolysis temperature, as shown in Fig. 7. The radicals could be detected above 900 K, and the concentration increased with increasing temperature, showing two peaks at about 1300 and 1800 K. The line width decreased with temperature, but turned to increase above 1800 K.

The radical species formed at temperatures lower than 1300 K are considered to be the Si-sited radicals as in the case of PCS. The radicals formed at higher temperatures than 1300 K should be assigned to the C-sited radicals because both their line width and  $g$ -factor are the same as those of the radicals formed in the PCS pyrolysis at high temperatures. The profile of the radical concentration is also similar to that of the  $H_2$  evolution, though the former is larger at high temperatures. It is indicated that the quantity of the radicals trapped in the pyrolyzed PCS and PCSZ is closely related to the  $H_2$  release.

Figure 8 shows the changes in XRD pattern of the pyrolyzed PCSZ with heat treatment temperature. The

original PCSZ showed diffraction peaks at about  $12^\circ$  and  $22^\circ$ . They disappeared and two peaks appeared at about  $35^\circ$  and  $70^\circ$ , as the heat treatment temperature increased. The structures of the pyrolyzed products were amorphous up to 1773 K. The diffraction peaks of  $\beta$ -SiC and  $Si_3N_4$  could be detected above 1773 K. In this temperature range, the third peak in the  $H_2$  evolution from PCSZ has finished as shown in Fig. 5. The peaks of  $Si_3N_4$  are not so clear as those of  $\beta$ -SiC during the pyrolysis in an argon atmosphere.

## Conclusions

The stepwise reactions in the pyrolysis process of organosilicon polymers are proposed. The analysis of the evolution gas species during pyrolysis indicates the types of chemical bond which were cleaved. Schematic representation of the chemical reaction accompanied by the gas evolutions and radical formations during the pyrolysis are summarized in Fig. 9. The cleavages of Si–H and Si– $CH_3$  bonds occur at the early stage of the pyrolysis, and those of N–H and C–H bonds follow them. The oxygen and the nitrogen atoms built in the inorganic amorphous network are eliminated as CO and  $N_2$  at the final stage of the pyrolysis. These bond cleavages form several kinds of radicals in the products. The radicals formed at the site of hydrogen atoms can be easily trapped in the product as compared with the radicals formed by the decomposition of the other chemical groups, such as Si– $CH_3$ , Si–O–, and Si–N=. The precipitation of microcrystals in amorphous matrix proceeds just after the decomposition of the C–H bond and is accompanied by the evolution of CO, or CO and  $N_2$  gases.

## References

- 1) T. F. Cooke, *J. Am. Ceram. Soc.*, **74**, 2959 (1991).
- 2) M. Narisawa and K. Okamura, "Chemical Processing of Ceramics," ed by B. I. Lee and E. J. A. Pope, Marcel Dekker, New York (1994), pp. 375–394.
- 3) E. Fizer and R. Gadow, *Am. Ceram. Soc. Bull.*, **65**, 326 (1986).
- 4) A. J. Caputo, D. P. Stinton, R. A. Lowden, and T. M. Besmann, *Am. Ceram. Soc. Bull.*, **66**, 368 (1987).
- 5) Y. Hasegawa and K. Okamura, *J. Mater. Sci.*, **18**, 3633 (1983).
- 6) E. Bouillon, F. Langlais, R. Pailler, R. Naslain, F. Cruege, P. V. Huong, J. C. Sarthan, A. Delpuech, C. Laffon, P. Lagarde, M. Monthieux, and A. Oberlin, *J. Mater. Sci.*, **26**, 1333 (1991).
- 7) O. Funayama, M. Arai, Y. Tashiro, H. Aoki, T. Suzuki, K. Tamura, H. Kaya, H. Nishii, and T. Isoda, *J. Ceram. Soc. Jpn.*, **98**, 104 (1990).
- 8) D. Bahloul, M. Pereira, P. Goursat, N. S. Choog Kwet Yive, and R. J. P. Corriu, *J. Am. Ceram. Soc.*, **76**, 1156 (1993).
- 9) D. Mocaer, R. Pailler, R. Naslain, C. Richard, J. P. Pillot, and J. Dounogues, *J. Mater. Sci.*, **28**, 2632 (1993).
- 10) T. Seguchi, M. Sugimoto, and K. Okamura, "Heat-

Resistant SiC-Fiber Synthesis and Reaction Mechanisms from Radiation-Cured Polycarbosilane Fiber," "6th European Conference on Composite Materials (EACM); High Temperature Ceramics Matrix Composites (HT-CMC1)," ed by R. Naslain, J. Lamon, and D. Doumeingts, Woodhead Publishing (1993), pp. 51—57.

11) M. Sugimoto, T. Shimoo, K. Okamura, and T. Seguchi, "Proc. of 1993 Powder Metallurgy World Congress (1993)," Abstr., p. 662.

12) T. Taki, *Polym. Prepr. Jpn.*, **42**, 3605 (1993).

13) K. Okamura, *Composites*, **18**, 107 (1987).

14) "Chemical Bond Energy," in "Kagaku Binran, Kiso-hen," revised 2nd ed, ed by Chem. Soc. Jpn., Maruzen, Tokyo (1975), Vol. 2, pp. 975—978.

15) T. Shimoo, M. Sugimoto, Y. Kakehi, and K. Okamura, *J. Jpn. Inst. Met., Sendai*, **55**, 294 (1991).

16) K. Tanaka, T. Koike, T. Yamabe, J. Yamauchi, Y. Deguchi, and S. Yata, *Phys. Rev. B*, **35**, 8368 (1987).

---